OA-pSDF BPOF의 특성 및 광학적 구현

正會員 任 鍾 太*　正會員 朴 成 鈞**　正會員 嚴 桂 旭***　正會員 朴 漢 奎****

The Characteristics and Optical Implementation of OA-pSDF BPOF

Jong Tae Ihm*, Seong Gyoon Park**, Joo Uk Um***,

Han Kyu Park**** *Regular Members*

要 約

본 논문에서는 이축 투사 합성 분리함수(OA-pSDF) 근거한 가간섭성 광상관 시스템을 해석하고 이를 광학적으로 구현하고, 사용된 성합필터는 전형적인 pSDF와 단일 기준 평면파를 다중화하여 합성하였다.

합성된 pSDF는 이진위상필터(BPOF)로 변환되어 고가의 공간광변조기 대신 실시간 광상관 시스템에 사용될 수 있도록 컴퓨터 홀로그램(CGH)으로 제작되었다.

특성시험에서 OA-pSDF는 변형불변 특성과 부분집합 영상의 분별에도 좋은 성능을 보임을 알 수 있었다.

시뮬레이션과 광실험에서 제안된 OA-pSDF BPOF는 기존 BPOF의 크기, 회전, 비동일 평면에서의 변위 등에 성능이 저하되는 단점을 극복하고 출력 평면상에서 주어진 위치에서의 상관값을 관측함으로써 클래스간의 분별 또는 동일 클래스로의 인식 등에 훌륭한 분별력을 가짐을 확인할 수 있었다.

ABSTRACT

In this paper, an coherent optical correlator system based on the off-axis projection synthetic discriminant funtion (OA-pSDF) was analyzed and implemented optically. The filter was synthesized by combining conventional pSDF with single reference plane wave multiplexing.

Synthesized pSDF were transformed to binary phase only filters(BPOFs) and fabricated as computer generated holograms(CGHs), which was used in the real time optical correlator system instead of using expensive spatial light modulators(SLMs).

From the characteristic test, it was found that OA-pSDF showed distortion invariance and good performances in discrminating subset images.

The proposed OA pSDF BPOF could overcome the limitations of conventional BPOFs ; that is distortion variance such as acale and rotation, especially out of plane variance.

* 한국이동통신(주) 중앙연구소
** 공주대학교 정보통신과
*** 한국전기통신공사 품질보증단
**** 인제대학교 전파공학과

1433

I. Introduction

Optical correlators are well known to be power ful systems and architectures that can recognize multiple occurrences of object in the presence of noise by the nature of high speed and parallel pro cessing. Optical systems using holographic mat ched spatial filters easily perform the correlation function.

The basic Vander Lugt correlator [1] employs a matched filter in the frequency plane. However, the performance of a correlator rapidly degrades as distortions are present in the input image. The synthetic discriminant function filter [2] and its variations[3,4] have advanced in decades of years to improve the performance of filters.

But the conventional projection synthetic dis criminant function(pSDF) has some limitations to be used in optical correlator: i.e., since the con ventional pSDF discriminates patterns in inter class discrimination or intraclass recognition prob lem by the relative correlation peak values or their combinations, if the classes to be classified increase, the number of filters also increases, so the physical filter dimension becomes larger or correlation peak level must ve divided into smal ler sub-levels which may make an ambiguous dic ision.

To solve these limitations, an off-axis pSDF (OA-pSDF)[5,6] which is constructed by combin ing conventional pSDF with angular multiplexing is suggested and implemented optically.

To improve optical efficiency of filters, de scribed filter is fabricated as binary phase only fil ter(BPOF)[7], and from which computer generat ed hologram(CGH) [8,9] is constructed to be used in the real time optical correlator.

II. Off-Axis pSDF

1. Unified pSDF Formulation

In most cases, pSDF synthesis contains inverse matrix operation. Pseudoinverse algorithm can be introduced to solve this problem efficiently [2].

Let a training image be denoted by $x_j^{(i)}$ where $i=1,2,......,K$ is the image class, K is the total number of classes, $j=1,2,.....,M_i$ is the image sam ple, and M_i is the total number of training images in the its class. $x_j^{(i)}$ is a column vector of lengeh N obtained by lexicographically scanning the train ing set images. All training images are columnwise ordered in a

$[N$ by $\sum_{i=1}^{k} M_i]$ matrix W : i.e.,

$$W = [x_1^{(1)} \cdots x_{M1}^{(1)},\ x_1^{(2)} \cdots x_{M2}^{(2)}, \cdots, x_1^{(k)} \cdots x_{Mk}^{(k)},] \quad (1)$$

In pSDF problem, the pseudoinverse method seeks a [K by N] linear transformation matrix S, such that the ith row vector of S will map all the sample training images into the ith row vector in a K dimensional decision space.

That is,

$$S \cdot W = U \quad (2)$$

where W is the training image data base matrix expressed by a [N by KM], and U is a [K by KM] orthogonal matrix.

In the lineat equations of Eq.(2) each row vec tor s_i of S, has N free variables, and therefore N training images are needed to determine s_i uniq uely. In the case of underdetermined problem whic h is $KM < N$ the minimum-norm solution of Eq. (2) is given by

$$S = U R^{-1} W^T. \quad (3)$$

where R is an image correlation matrix for all the training images, and T denotes the transpose operation [10].

The linear mapping transformation is related to the inverse of the image correlation matrix R. The image correlation matrix R is a [KM by KM] matrix (KM being the rank of R and the number of linearly independent training images), there fore the inverse natrix R^{-1} exists.

Let row vector of length N be $s_i(i=1,2,\cdots K)$, Eq.(3) can be rewritten as

$$S = \begin{bmatrix} s_1 \\ s_2 \\ \vdots \\ s_k \end{bmatrix} \tag{4}$$

Form Eq.(4), it is recognized that each s_i is linear mapping of each class or pSDF for each class.

2. Angular Multiplexing of pSDF

The Vander Lugt filter of a function $f(x,y)$, created through conventional holographic techniques, yields the transmittance function, i.e.,

$$H(u,v) = A^2 + |F(u,v)|^2 + A \cdot F(u,v)\exp[i2\pi(au+bv)] \\ + A \cdot F^*(u,v)\exp[-i2\pi(au+bv)] \tag{5}$$

where $F(u,v)$ is the Fourier transform of $f(x,y)$, $A\exp[-i2\pi(au+bv)]$ is the off-axis reference wave used to create the hologram, and $*$ denotes complex conjugate of a function.

From Eq.(5), only the fourth term plays an important role in filter synthesis, and is needed.

In this case, substituting each $s_i(x,y)$ of Eq.(4) into $f(x,y)$ of Eq.(5) can result in OA-pSDF; that is the desired OA-pSDF $J(u,v)$ is described by

$$J(u,v) = [\sum_{i=1}^{k} k_i \{s_i(x,y)\}\exp[i2\pi(a_iu - b_iv)]]^*, \tag{6}$$

where $J(u,v) = \mathcal{F}\{J(x,y)\}$, and a_i and b_i are the direction cosines of the ith plane wave carrier, and k_i denotes amplitude of ith plane wave carrier and can be chosen such that the autocorrelation peaks have the same amplitude. And properly chosen, correlation peaks for each class can be separated in the output correlation plane by properly choosing a_i and b_i.

III. Experiments and Discussions

1. Set-up for Experiments

The fundamental set-up for computer simulation and optical verification is as shown in Fig.1

The system in Fig.1 can reduce the system length by a factor of 2-3 with respect to the conventional 4-f system by introducing concave lens.[11]
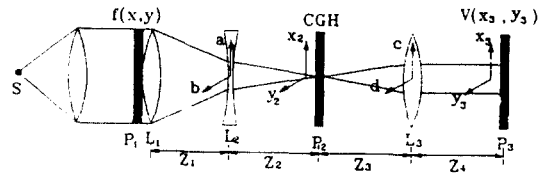

Fig. 1. Set-up for experiments

In this case, the calulated focal length f which will be determined in designing CGH and may be unmatched to focal length of the common lenses, is 1741.37mm, and so the conventional system with the length of 4-f is $1741.37 \times 4 = 6965.48$mm. But using the suggested system as Fig..1, the focal length can be varied by combination of concave and convex lens. As a result, the total length of suggested system is 2962.816mm.

2. Computer Simulations

2.1 Characteristics of OA-pSDF BPOF

The conventional BPOF(CBPOF) shows high output S/N, but has a minor effect that can not discriminate similar images between subset ones. For example, as shown in Fig.2 character F is a subset image of character E, and so CBPOFs can show very high cross-correlation peak, about more than 70% of auto-correlation.

But OA-pBPOF has an improved performance to compensate this minor effect of CBPOFs. The input patterns for simulations are composed 16×11 pixels.

(a) Input-E   (b) Input-F

Fig. 2. Input patterns 'E' and 'F'

The computer simulation results are shown in Fig.3 and Fig.4 for CBPOF, and OA-pSDF BPOF, respectively.

1435

To compare performance of filters, a parameter Q which means that the smaller the value is, the better the performance is, can be defined as

$$Q = \frac{\text{cross correlation value}}{\text{auto-correlation peak value}} \qquad (7)$$

table. 1. Parameter Q of CBPOF and OA pSDF BPOF

Input \\ Filter	CBPOF	OA pSDF
E	0.19	0.25
F	0.71	0.41

Parameter Q indicates that filter with smaller Q value can discriminate subset images more effectively.

From Fig.3, Fig.4 and Table 1, it is noted that OA pSDF can discriminate between sub pattern images more efficiently than CBPOF.

Another characteristic of OA pSDF is that it can recognize distortion images of original training images.

To show this characteristic, two class problem is considered and each class has five training images. The patterns used and two of correlation
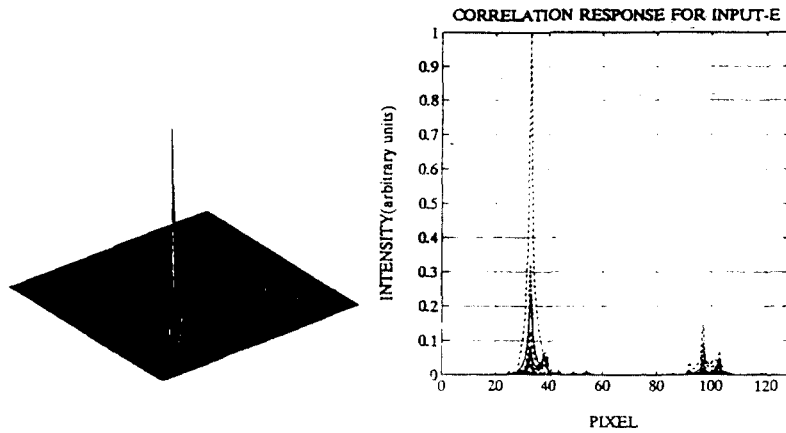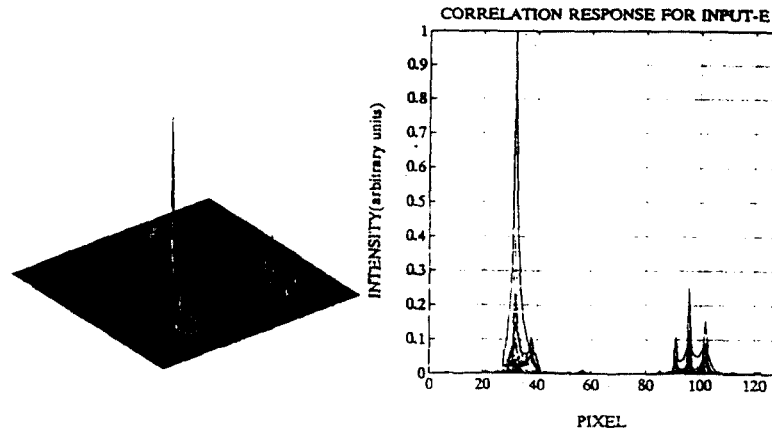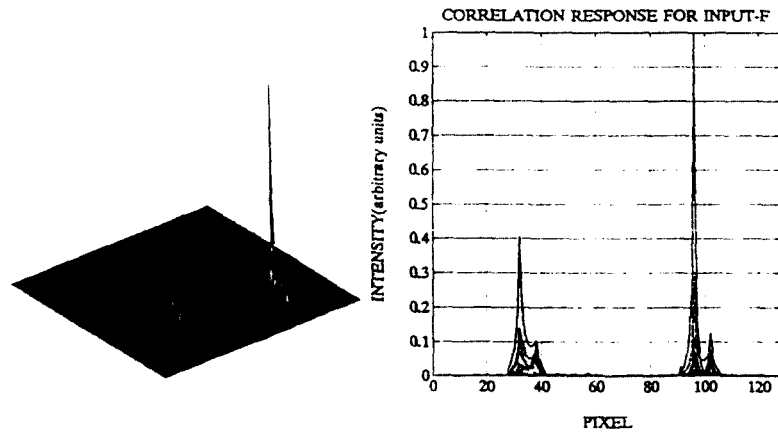
(a) Correlation response for input-E
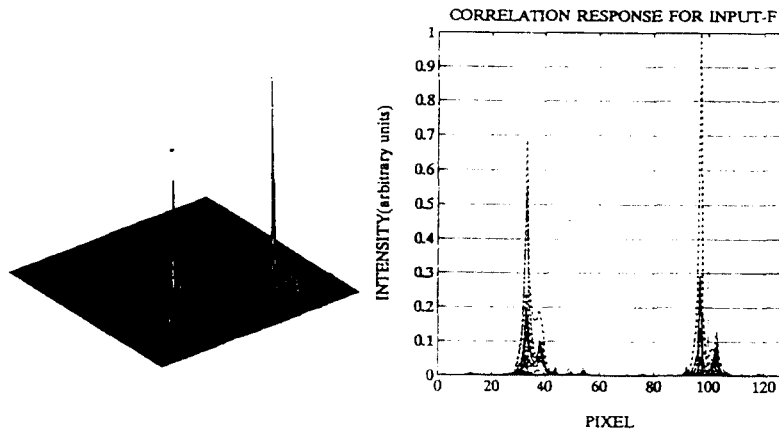
(b) Correlation response for input-F

Fig. 3. Computer simulation results for CBPOF

(a) Correlation response for input-E

(b) Correlation response for input-F

Fig. 4. Computer simulation results for OA-pSDF BPOF

(a) Training images for class-A

(b) Training images for class-B

Fig. 5. Training images

outputs are shown in Fig.5 and Fig.6

Each one of the input patterns in Fig.5 and 6 is composed of 16×11 pixels and the locations of output correlation peaks are (92, 32) for class-A and (96, 96) for class-B for 128×128 output correlation plane size.

2.2 Correlation Responses of OA-pSDF BPOF

The input patterns used for computer simulations are composed of 16×16 pixel images, which are shown in Fig.7
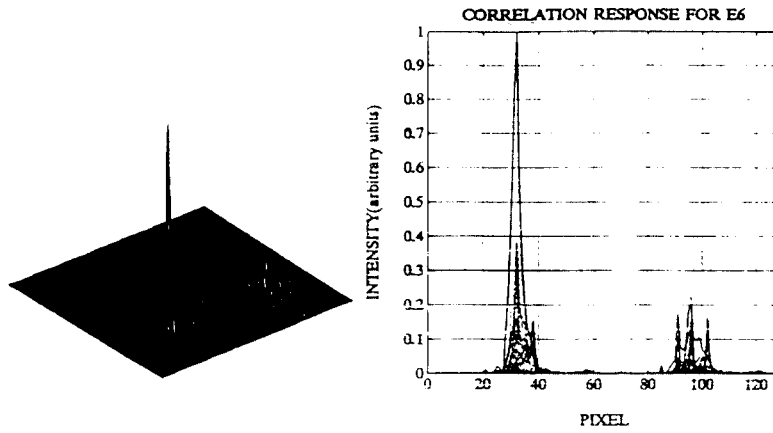
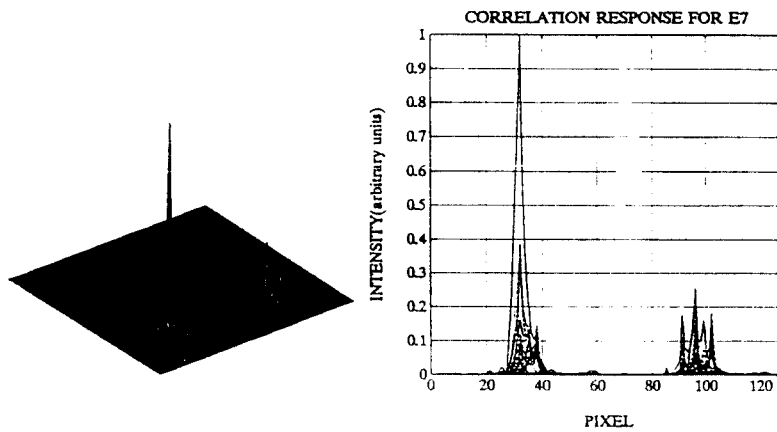In Fig.1, input plane, filter plane and corre-

1437

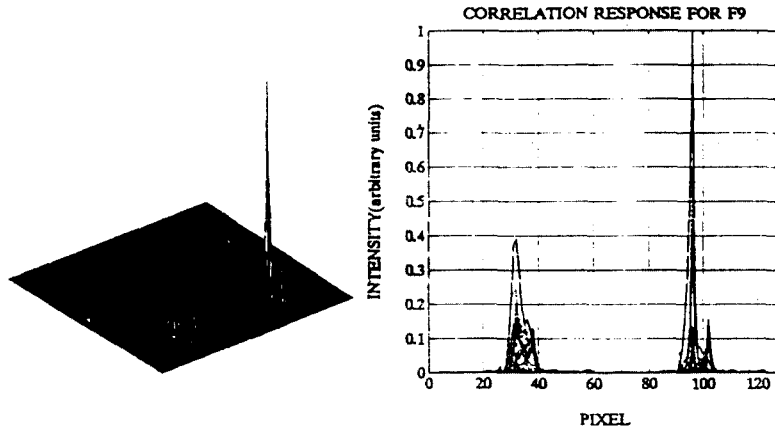(a) Distorted images for class-A

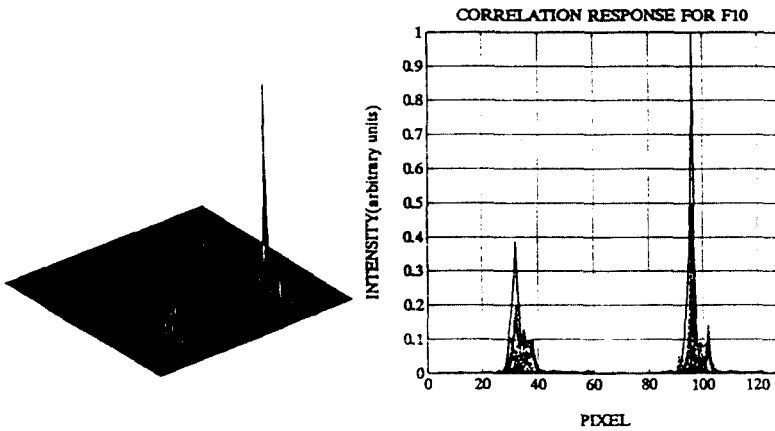(b) Distorted images for class-B

(c) Correlation response for E6

(d) Correlation response for E7

(e) Correlation response for F9

(f) Correlation response for F10

Fig. 6. Distorted input patterns and correlation outputs
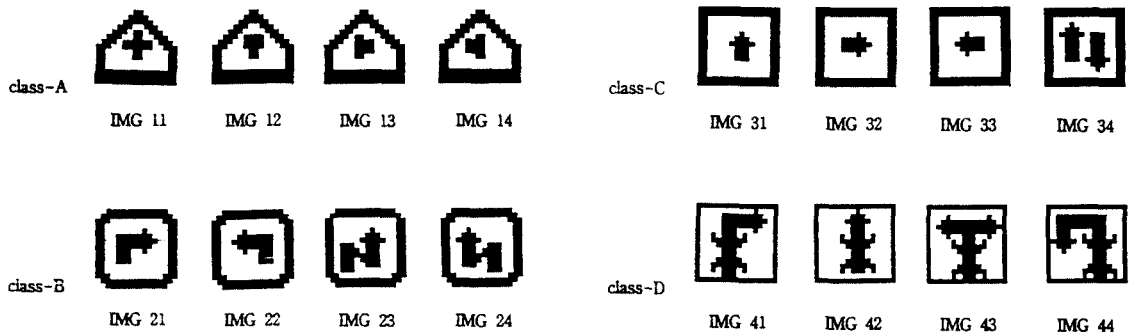

class-A   IMG 11   IMG 12   IMG 13   IMG 14

class-C   IMG 31   IMG 32   IMG 33   IMG 34

class-B   IMG 21   IMG 22   IMG 23   IMG 24

class-D   IMG 41   IMG 42   IMG 43   IMG 44

Fig. 7. training images

1439

lation plane, each plane consists of 128×128 pixels.

The simulation is performed for the case of inter and intra problems; i.e. the designed filter must discriminate input patterns between classes and recognize input patterns belonged to any one class as same class. The correlation peak location designated are (96,16), (96,48), (96,80), and (96, 112) of correlation plane for class A class B, class-C, and class-D, respectively. If some regions of output correlation plane are defined as follows; e.

region A : 32×32 pixels centered at (90, 16)
region B : 32×32 pixels centered at (90, 48)
region C : 32×32 pixels centered at (90, 80)
region D : 32×32 pixels centered at (90, 112)

discriminant parameter K can be defined as

$$K = \frac{T - F}{T} \tag{8}$$

when T means maximum correlation peak value at the designated location in the region which has the desired peak value, and F means the average value of correlation peaks which are belonged to the rest of output plane except the plane containing T.

From Eq.(8) it is noted that K having value close to 1 shows better recognition capability. Table. 2 shows correlation peak values of each region A, B, C, D and Table 3 summarizes K parameter.

In optical set-up shown in Fig.1, the focal lengths of lenses, are 600mm for L_2, -100mm for

table. 2. Maximum correlation peak values of region A, B, C, D

Input \ Region		A	B	C	D
Class A	IMG 11	1	0.1767	0.1332	0.0662
	IMG 12	1	0.1644	0.1237	0.0683
	IMG 13	1	0.1403	0.1045	0.0720
	IMG 14	1	0.1484	0.1151	0.0634
Class B	IMG 21	0.1150	1	0.1357	0.0834
	IMG 22	0.1156	1	0.1518	0.0548
	IMG 23	0.11740	1	0.1516	0.0633
	IMG 24	0.1131	1	0.1691	0.0502
Class C	IMG 31	0.0620	0.1521	1	0.0522
	IMG 32	0.0796	0.1673	1	0.0549
	IMG 33	0.0803	0.1473	1	0.0593
	IMG 34	0.1612	0.1971	1	0.0782
Class D	IMG 41	0.0788	0.1130	0.1189	1
	IMG 42	0.1237	0.0610	0.0988	1
	IMG 43	0.1753	0.1411	0.1527	1
	IMG 44	0.1051	0.0968	0.1310	1

concave L_3, and 550mm for L_1, and $Z_1 = 534.456$mm, $Z_2 = 190.23$mm, $Z_3 = 550$mm, and $Z_1 = 1652.13$mm are obtained. Because of the aberration effects of concave lens such as coma, astigmation etc., the shorter the length Z_2 between lens L_3 and filter plane is, the better experimental results can be obtained. The output correlation patterns are obtained using CCD camera.

IV. Discussions

The results of interest fell in two categories:(1) characteristics of OA-pSDF

table. 3. K parameter

Input	Class A				Class B			
	IMG 11	IMG 22	IMG 33	IMG 44	IMG 21	IMG 22	IMG 23	IMG 24
K	0.8746	0.8812	0.8944	0.8910	0.8886	0.8926	0.8904	0.8972
Input	Class C				Class-D			
	IMG 31	IMG 32	IMG 33	IMG 34	IMG 41	IMG 42	IMG 43	IMG 44
K	0.9111	0.8994	0.9044	0.8545	0.8964	0.9055	0.8436	0.8890

BPOF(2) computer simulation and bench test for OA-pSDF BPOF.

In the simulations of characteristics of OA-pSDF BPOF, two points of view are considered. One is to test the capability of subset image discrimination and the other is distortion invariance. From Fig.3, CBPOF shows resonable correlation peak located at desired position for input pattern 'E', but ambiguous correlation outputs for input pattern 'F'. In the case of character 'F', the correlation peak difference between the position for input 'E' and that for input 'F', is very small; i.e. Q value is 0.71, and so CBPOF may confuse whether the input pattern is character 'E' or 'F'.

However, as shown in Table 1, OA-pSDF BPOF can reduce the Q value from 0.71 to 0.41, and shows improved performance which results in eliminating incorrection recongnition. To test distortion invariance, some training images of chsrscter E for class A and chacter F for class B are used for training.

In Fig.5, there are training images, and distorted images and their correlation respones are shown in Fig.6 Comparing these results show no differences in their correlation responses. From this it is pointed out proposed that OA-pSDF BPOF

can recognize distorted patterns which do not belong to the training images, and has distortion invariance characteristics.

In the case of OA-pSDF BPOF simulation, as shown in Fig.8, sharp correlation peak can be obtained separately at the desired correlation positions such as location (96,16) of correlation plane for class-A, location (96, 48) for class-B, location (96, 80) for class-C, and location (96,112) for class-D. From Table 3, it is seen that large discriminant factor Ks for each input to be classified are obtained properly. The value of Ks is close to 0.9 or more in most cases, and it is found that proposed OA-pSDF BPOF has high discriminant capability.

In optical expriments, owing to the nature of the BPOF, unwanted noise terms are appeared at the opposite side centered at the dc terms as shown in Fig.10. Comparing simulation results in Fig.8 with bench test in Fig.10, there exist some differences between them. This seems to be the effects of nonlinear transformation during binarization procedure of making BPOF from POF and approximate phase encoding of CGH rather than exact 'π' and '0' phase encoding for '1' and '-1', respectively. The phase encoding problem can be solved if SLM is to be used for real time CGH.
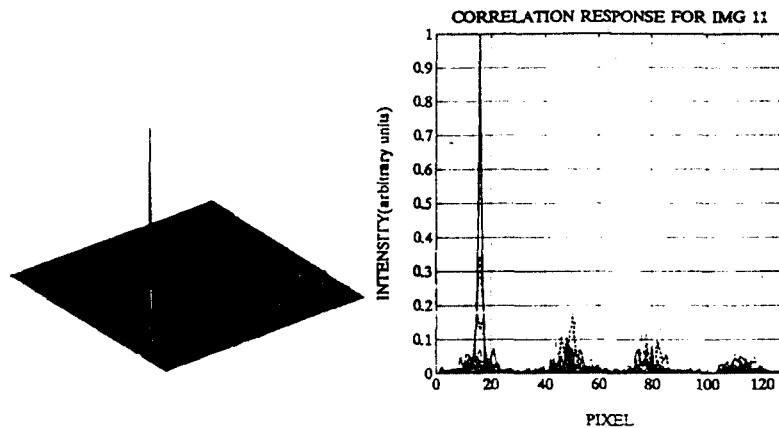
(a) Correlation response for input IMG 11

1441
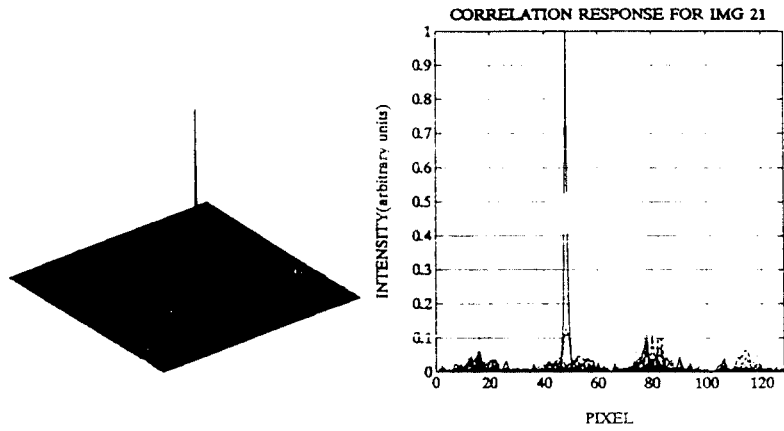
(b) Correlation response for input IMG 21
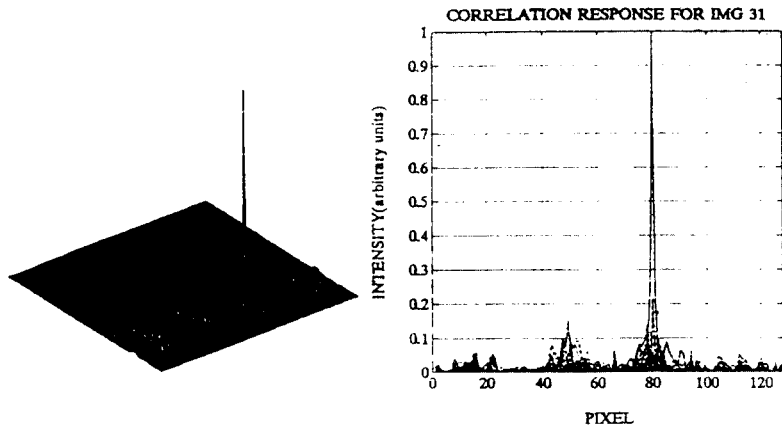
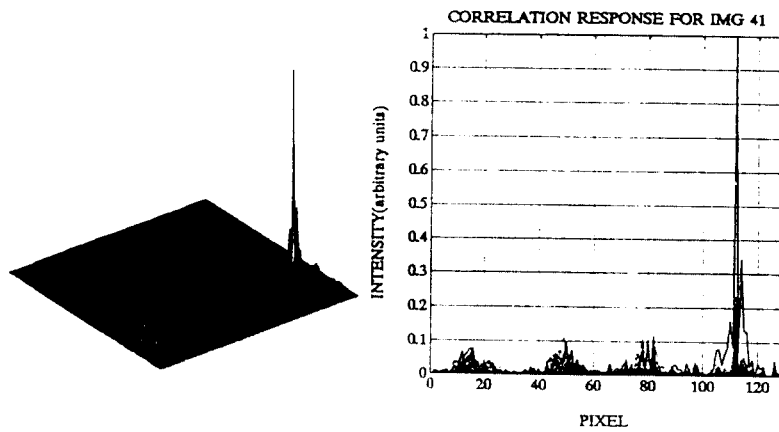(c) Correlation response for input IMG 31

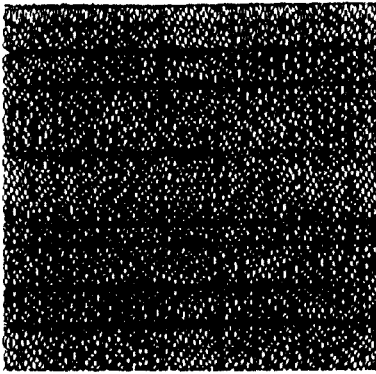Fig. 8. Correlation outputs for input pattern

Fig. 9. Designed CGH patterns

V. Conclusions

In this paper, an coherent optical correlator based on the multiplexed pSDF is analyzed and implemented. The proposed OA-pSDF is synthesized by combining conventional pSDF with single reference beam multiplexing. Synthesized pSDFs in this paper are tranformed to BPOFs and fabricated as Lee type CGH which is frequently used in the real time optical correlator system instead of expensive spatial light modulators(SLMs).

The designed OA-pSDF BPOF shows distortion

(a) For IMG 11　　(b) For IMG 12　　(c) For IMG 13　　(d) For IMG 14

(e) For IMG 21　　(f) For IMG 22　　(g) For IMG 23　　(h) For IMG 24

(i) For IMG 31　　(j) For IMG 32　　(k) For IMG 33　　(l) For IMG 34

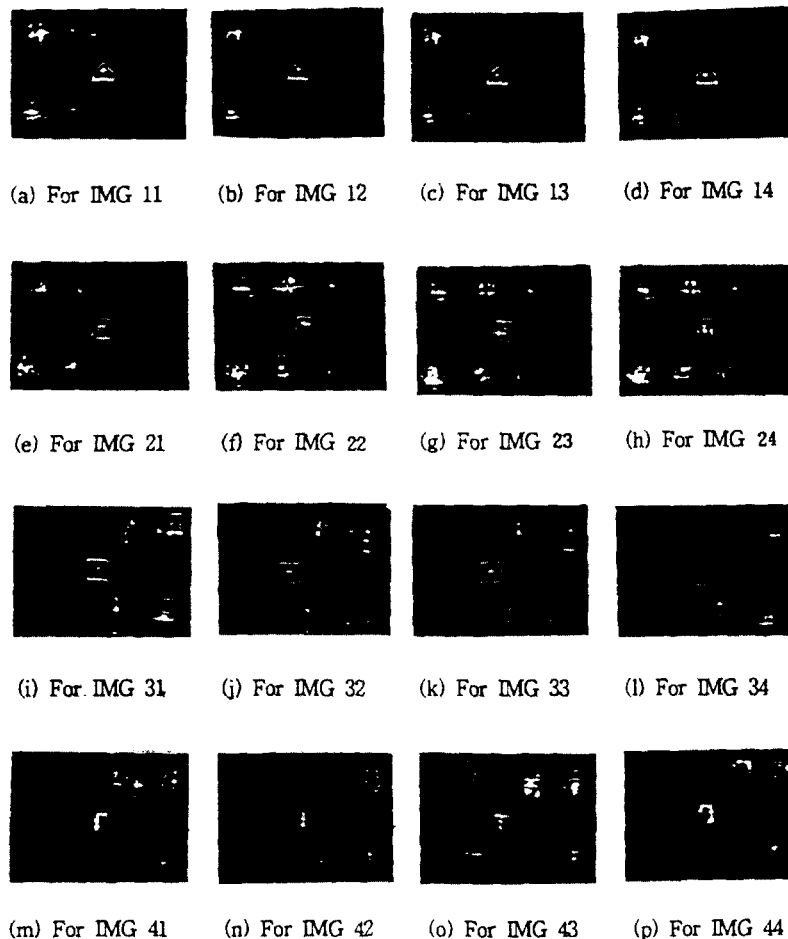(m) For IMG 41　　(n) For IMG 42　　(o) For IMG 43　　(p) For IMG 44

Fig. 10. Optical correlator outputs of OA-pSDF BPOF

invariance and good performances in discriminat
ing subset images, which are impossible for con
ventional BPOFs.

The proposed OA-pSDF BPOF can overcome
the limitations of conventional pSDFs which dis
criminate patterns by relative correlation peak
values or combinations physical size of the filter
also increases in proportional to the number of fil
ters to be combined, or very sensitive photodet
ector and threshold device is needed to dis
tinguish correlation peaks at their own designated
location in the output correlation plane, it is very
easy and clear to discriminate patterns in the
case of interclass discrimination, intraclass recog
nition, or mixed problems.

REFERENCES

1. A. Vander Lugt, "Signal Detection by Complex
   Spatial Filtering", IEEE Trans. Inform. The
   ory, Vol. IT-10, pp. 139, 1964.

2. D.Casasent, "Unified Synthetic Discriminant
   Function Computational Formulation", Appl.
   Opt., Vol.23, No.10, pp. 1620~1627, 1984.

3. D. Casasent and W.T. Chang, "Correlation
   Synthetic Discriminant Functions", Appl. Opt.,
   Vol.25, No.14, pp. 2343~2350, 1986.

4. A.Mahalanobis and D.P.Casasent, "Perform
   ance Evaluation of Minimum Average Corre
   lation Energy Filters", Appl. Opt., 30, No.5,
   pp.561~572, 1991.

5. J.T.Ihm, H.K.Park, M.S.Kim, and S.I.Kim,
   "Off axis pSDF Spatial Filter for Pattern Clas
   sification", Jour. of OSK., Vol.2, No.2, pp.83~
   88, 1991.

6. J.T.Ihm, S.G.Gil and H.K.Park, "Reference
   Beam Encoded SDF Spatial Matched Filter For
   Pattern Classifier", Proc. of ICCT 1992
   (china), Vol.2~2, pp. 23.13.1~23.13.4, 1992.

7. J.L.Horner and P.D.Gianino, "Applying the
   Phase Only Filter Concept to the Synthetic Dis
   criminant Function Correlation Filter", Appl.
   Opt., Vol.24, No.6, pp. 851~855, 1985.

8. J.T.Ihm, R.S.Kim, W.H.Kwon, H.K.Park,
   "Real-Time Deformation Invariant Optical Cor
   relator Using Photorefracative Medium", Proc.
   of JC-MECOD., 1988.

9. W.H.Lee, "Binary Computer-Generated Hol
   ograms", Appl. Opt., Vol.19, No.21, pp. 361~
   3669, 1979.

10. W.K.Pratt, Digital Image Processing (Wiley,
    New York, 1978). pp. 206~207.

11. D.L.Rannery, A.M.Biemacki, J.S.Loomis, and
    S.L.Cartwright, "Real-time coherent correl
    ator using binary magnetooptic spatial light
    modulators at input and Fourier planes",
    Appl. Opt. Vol.25, No.1, pp.466, 1986.
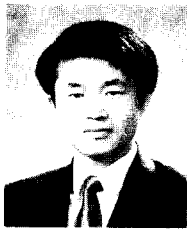
任 鍾 太(Jong Tae Ihm) 정회원
1960년 10월 2일생
1986년 2월 : 연세대학교 전자공학
과(공학사)
1988년 2월 : 연세대학교 대학원 전
자공학과(공학석사)
1993년 2월 : 연세대학교 대학원 전
자공학과(공학박사)
1993년 11월 ~ 현재 : 한국이동통신(주) 중앙연구소
전파환경 연구팀 팀장
※주관심분야 : 광정보처리, 안테나 및 이동통신 전파전파
특성, 안테나 측정 및 EMC

朴 成 鈞(Seong Gyoon Park) 정회원
1962년 1월 1일생
1985년 2월 : 연세대학교 전자공학
과(공학사)
1987년 2월 : 연세대학교 대학원 전
자공학과(공학석사)
1994년 2월 : 연세대학교 대학원 전
자공학과(공학박사)
1987년 4월 ~ 1989년 7월 : 삼성전자 정보통신 연구소 연구
원 근무
1994년 3월 ~ 1994년 8월 : 한국전자통신연구소 위촉연구원
1994년 9월 ~ 현재 : 공주대학교 정보통신과 교수
※주관심분야 : 광전자, 이동통신

嚴 柱 旭(Joo Uk Um) 정회원
1960년 3월 17일생
1982년 2월 : 연세대학교 전자공학
과(공학사)
1984년 2월 : 연세대학교 대학원 전
자공학과(공학석사)
1992년 3월 ~ 현재 : 연세대학교 대학
원 전자공학과(박사과
정)
1985년 5월 ~ 현재 : 한국전기통신공사 품질보증단 선임 연
구원
※주관심분야 : 광전송시스템, 초고주파 광학

朴 漢 奎(Han Kyu Park) 正會員
1941年 6月 21日生
1964年 2月 : 延世大學校 電氣工學
科 卒業
1968年 2月 : 延世大學校 大學院 電
氣工學科 卒業(工學碩
士)
1973年 : 불란서 파리大學校(소르본
느大學校) 博士課程修了
(DEA)
1975年 : 불란서 파리6대학(ph.D)
1976年 ~ 現在 : 延世大學校 電子工學科 教授